EXPERIMENTAL VERIFICATION OF OSCILLATORY PHENOMENA IN HEAT TRANSFER IN A COMMUNICATING CHANNELS GEOMETRY

C. V. Herman*, F. Mayinger* and D. P. Sekulić**

* Lehrstuhl A für Thermodynamik, TU München, München, Germany
** Institut za termoenergetiku i procesnu tehniku
Univerzitet u Novom Sadu, Novi Sad, Yugoslavia

ABSTRACT

Forced convection heat transfer in laminar and transitional flow in a communicating channels geometry is investigated experimentally. The instationary temperature fields were visualized by means of real time holographic interferometry. The test section is a parallel plate duct with near adiabatic top and bottom walls and a series of heated plates positioned in the central plane of the duct with uniform heat flux imposed on the plates. The working fluid is air. In hydrodynamically fully developed flow conditions, the temperature fields on a heated plate — periodicity element — were visualized and filmed using high speed cinematography with film velocities up to 600 picture frames per second. The experiments verified the oscillatory nature of the fluid flow and heat transfer phenomena. Two representative regimes, Re = 366, corresponding to the situation of the onset of oscillations and Re = 593.5, for which oscillations are intensive, are discussed.

INTRODUCTION

In order to improve the performance of compact heat exchangers, high-power-density electronic equipment etc., the heat transfer surfaces are frequently equipped with fins, and the analysis of their performance has been the subject of many research efforts [1]. These devices usually operate at low or moderate Reynolds numbers. The overall heat transfer and pressure drop performances of the complex geometries used in compact heat exchangers have been treated in numerous publications [2]. The data available in the literature provide the design engineers with the necessary information for the solution of practical problems, but a need for good insight on a physical level into the fundamental physical phenomena bringing the augmentation of heat transfer — in order to effectively exploit these effects — is still present.

The geometry investigated in this work is presented schematically in figure 1, and it is a heat transfer surface periodically interrupted in the streamwise direction as in the rectangular plate-fin, offset-fin, offset strip-fin and the louvered fin configurations [2].

The experimental channel is a parallel plate duct with rectangular cross section (height h + a + h = 0.025 m, width w = 0.15 m and other dimensions indicated in figure 1) with the characteristic nondimensional parameters: (i) separation between the channels a/(h/2) = 1, (ii) periodicity length L/(h/2) = 8 and (iii) the groove width l/(h/2) = 3. The model fins are represented with a succession of parallel plate segments — they can analogously be viewed as a periodically interrupted surface — situated in the medial plane of the parallel plate duct. The working fluid is air, and the direction of air flow is indicated in figure 1 and figure 2. The top and bottom plates are near adiabatic and the thermal boundary conditions on the heated plates are characterized by uniform heat flux. The experimental arrangement consists of ten heated plates, thus at sufficient downstream distance a special form of fully developed flow regime is established with periodically repeating flow patterns. The measurements described in this paper were performed on the ninth heated segment.

There are many publications dealing with heat transfer and fluid flow on a single flat plate, two flat plates and plate arrays in different arrangements and on grooved geometries, also related to the communicating channels. Here, some of the references related to the subject of the paper will be discussed briefly. Cur and Sparrow (1979) [3] measured the developing and fully developed heat transfer coefficients along a periodically interrupted surface and investigated the influence of plate thickness on the heat transfer augmentation. They used the naphthalene sublimation technique for mass transfer experiments,

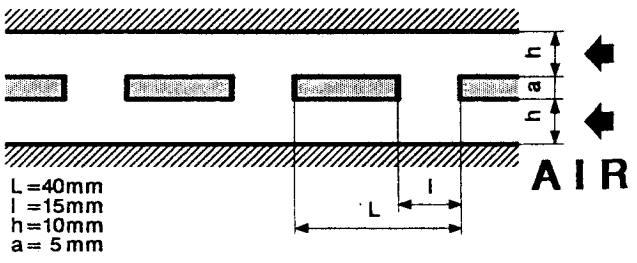

Fig. 1 Schematic of the investigated geometry

Experimental Heat Transfer, Fluid Mechanics, and Thermodynamics 1991
J.F. Keffer, R.K. Shah, and E.N. Ganić, Editors

and mass transfer results were then converted into heat transfer values using the analogy between the two processes. Kurosaki et al. (1988) [4] experimentally studied heat transfer from parallel louvered fins by means of laser holographic interferometry and visualized isotherms for various louver arrangements. The results of the experiments indicated that the performance of heat exchangers may significantly be improved by choosing appropriate arrangements of louvers. The instationary character of the heat transfer process was not considered. Shiina et al. (1988) [5] experimentally analysed the effect of spacers positioned in the central plane of a rectangular channel on the forced convective heat transfer. They measured local heat transfer coefficients and static pressure drop distributions. Wall temperature measurements were obtained by thermocouples. Mochizuki and Yagi (1980) [6] visualized and measured the instationary flow patterns and the frequencies of vortex shedding on a series of staggered arrays for a wide range of Reynolds numbers. However, most of the experimental data in the above references is confined to the time average heat transfer analysis.

Amon (1988) [7] and Amon and Mikić (1989) [8], (1990) [9] numerically investigated flow patterns and heat transfer enhancement in self sustained oscillatory flows in periodically grooved channels (a geometry essentially analogous to the one treated in this work — in the communicating channels the bottom wall of the grooved geometry is removed and communication between the channels is allowed) and in communicating channels with base geometries corresponding to the nondimensional periodicity length L/(h/2) = 5, groove width l/(h/2) = 3 and the separation between the channels a/(h/2) = 1 and 1.68 (applying the definitions of a and h used in this paper). The thermal boundary conditions were given by adiabatic plane surfaces in the grooved channel and the communicating channels geometry and with uniform heat flux on the grooved surface and on the heated plates. Flow patterns and velocity fields were presented for the fully developed flow situation and heat transfer was investigated for thermally fully developed domains. An increase of heat transfer of factor 3 was found for the same power dissipation in supercritical communicating channel flows compared with results obtained for flat channels. They found that oscillatory flows are optimal regarding pumping power.

The objective of the present work is the visualization and the qualitative analysis of the instationary temperature fields in the communicating channels geometry. This was achieved by means of real time holographic interferometry. The isotherms were visualized using the infinite fringe field arrangement and were recorded by high speed cinematography with film velocities up to 600 picture frames per second. Thus elements of the instationary phenomenon were registered, providing insight into the complex physical process of heat transfer in communcating channels. Also, pressure drop data on the test section is presented.

THE EXPERIMENTAL SETUP

The experimental setup used in the heat transfer analysis in the communicating channels geometry is presented schematically in figure 2. The experimental channel consists of the entry section, the test section itself and the exit section, and it is positioned horizontally. The entry section is a 0.3 m long, 0.15 m wide (its width corresponds to the length transilluminated by laser light) and 0.025 m high parallel plate duct with a screen at the entrance of the section. The working fluid, air, enters the channel through a funnel-shaped entrance to reduce effects of entrance drag. The direction of air flow is indicated by arrows.

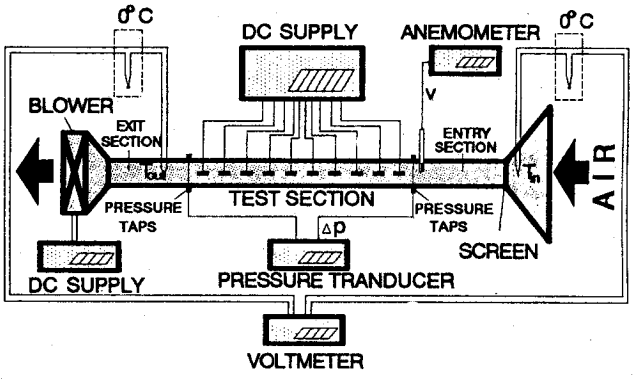

Fig. 2 Schematic of the experimental setup

The **test section** is 0.5 m long — its cross section is identical to that of the entry section — with a pair of grooves along the top and bottom plates which carry the side windows. The viewing window, the length of it matching the diameter of the expanded laser beam (78 mm), supports two of the ten heated plates positioned in the medial plane of the test duct. It is manufactured of glass to avoid influence of the window material on the interferometric image. Precisely bored holes accept the supporting sticks of the heated plates. By using glass plates with varying positions of the supporting holes, the distance between the plates can be varied. Outside of the viewing region the copper plates are carried by plexiglass holders. Here, the distance between the plates can be varied by varying the dimensions of the intermediate elements also manufactured of plexiglass. The test section can accept ten heated copper plates. The plane of the test section can precisely be defined by a three point adjustment. The temperature of the top wall of the test section is monitored by 17 nickelchrom-constanten thermocouples to provide additional reference temperature values, apart from the measurements on the heated plates.

The **exit section** is 0.3 m long, and it carries a blower operating in suction mode and creating the air flow. The flow velocity is varied by changing the dc supply voltage of the blower. Four pressure taps of 0.0001 m in diameter are located in each of the flanges between the entry and the test sections and between the test section and exit sec-

tion. They allow for pressure drop measurements on the test section. A pressure transducer Setra Series 239, calibrated by a Betz manometer was used for pressure drop measurements on the test section.

The structure of the heated copper plates is presented schematically in figure 3. Each plate is 144 mm long, 25 mm wide and 5 mm thick, and it is manufactured of two identical 2.5 mm thick halves. The sandwich structure encloses the electric heater foil. Material was removed from the contact surface of the copper plates to provide room for the heater foil with the current supply wires and for the thermocouple wires. In the outer surface of the top and bottom plates, two constantan-manganin 0.1 mm diameter thermocouples were integrated — their positions are indicated in figure 3 — and conducted along the plate to leave it at the same location as the power supply wires. The thermocouples allow for accurate measurements of plate temperatures giving reference temperature values for the interpretation of interferometric images. The sandwich structure was joined with glue. The desired temperature of the heated plates was achieved by varying the dc supply voltage of the heater foil.

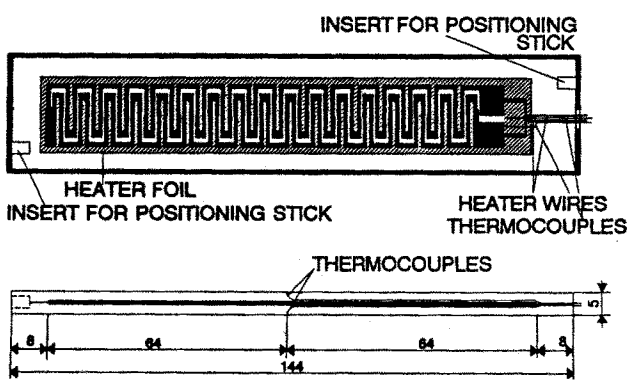

Fig. 3 Schematic of the heated copper plates

The temperature increase along the test section (T_{out} - T_{in}, figure 2) was measured by two batteries of nickelchrom-constantan thermocouples. Each battery consists of five thermocouples connected in series and distributed over the cross sectional area, providing average temperature values and yielding amplified emf for enhanced accuracy.

Air flow velocity profile measurements at the end of the entry section at three different cross sectional locations were obtained by a Schiltknecht hot wire anemometer thermo-air type 442. The anemometer measurements were calibrated by a rotameter.

THE EXPERIMENTAL METHOD

In the analysis of the instationary heat transfer process in the communicating channels geometry, the experimental method of holographic interferometry was selected. This method offers unique advantages in the study of high speed heat transfer processes ([10], [11], [12], [13]); without disturbing the investigated physical phenomenon it enables visualization and quantitative measurements of temperature fields with high spatial and temporal resolutions.

The method of interferometry and holography in heat transfer measurements has been treated in detail in the literature ([14], [15], [16]). The optical setup used in the experiments described in this paper is presented schematically in figure 4, and it corresponds to the setup described in the literature [15], with locations of the optical components dictated by the investigated geometry and the length of the experimental channel. Additional mirrors enhance the degrees of freedom in the adjustment of the optical arrangement in the range of the coherence length of the light source.

A He-Ne laser with $\lambda = 632.8$ nm, 30 mW power and 20 cm coherence length was used as light source and it was positioned on the optical table together with the optical components in order to keep the optical arrangement

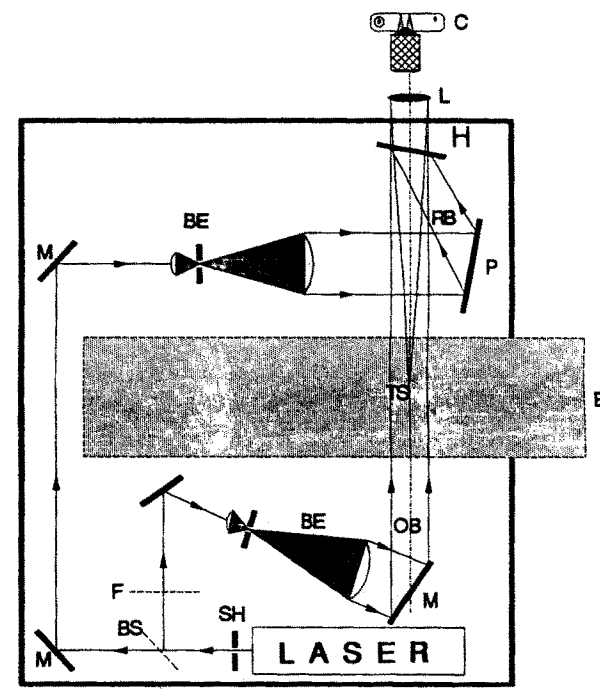

SH -	Shutter	L -	Imaging lens
M -	Mirror	C -	Camera
F -	Filter	T -	Optical table
BS -	Beam splitter	RB -	Reference beam
BE -	Beam expander	OB -	Object beam
P -	Mirror with piezo elements	TS -	Test section
HP -	Holographic plate	EC -	Experimental channel

Fig. 4 Schematic of the optical arrangement for holographic interferometry used in the investigation of heat transfer in the communicating channel geometry

as compact as possible. This was necessary in order to compensate for the relatively low power of the laser light source contrasted to the extremely short illumination times needed for high speed cinematography.

In the experiments, the real-time method was used. First the reference state of the process (experimental setup at ambient temperature) was recorded on the holographic plate. The holographic plate was then developed, bleached, dried and, after the processing, accurately repositioned into its original position using a precision plate holder. Then the investigated phenomenon was activated by the activation of the heaters in the heated copper plates and the blower. The high speed recordings were obtained with film velocities form 150 to 600 picture frames per second and the recording interval lasted approximately 5 s per state, corresponding to a total of maximum 3000 picture frames per state. By using the real time technique, in holographic interferometry high temporal resolutions can be achieved, limited only by the sensitivity of the photographic material and the mechanical limitations of the film transport velocity.

The high speed films enable the evaluation of oscillatory instationary temperature fields, while when observing the interferograms with the naked eye, only a mildly unsteady vibrating character of the image indicated towards the instationary nature of the process.

RESULTS AND DISCUSSION

Experimental Parameters

High speed recordings of the temperature fields in the communicating channels geometry were obtained for a set of operating parameters. Flow conditions in the experiments were specified by the Reynolds number Re, which has been defined as

$$\mathrm{Re} = \frac{3}{2}\,\frac{v_m\,(h/2)}{\nu}. \qquad (1)$$

Flow velocity measurements indicated approximately parabolic velocity profiles at the beginning of the test section. The selected channel aspect ratio h : w = 1 : 15 allows for a two dimensional flow approximation.

The thermal boundary conditions were defined by uniform heat flux on the heated plates and near adiabatic top and bottom walls of the test section. Numerical calculations and interferometric visualizations of the temperature fields of the heated plates from different viewing directions have proved that good isothermal conditions were present at the surface of each plate, which is significant for the accuracy of the evaluation of interferometric images. Thus essentially two dimensional temperature fields can be assumed.

Experimental runs were performed for Reynolds numbers in the range from Re = 120 to Re = 600. The electric power supported to the heaters was varied from 0.044 to 0.133 W/cm^2 (plate surface) — increasing with increasing air flow velocities, in order to obtain sufficient number of interference fringes for the quantitative evaluation of the interferograms. The high speed images were recorded on the ninth plate (the leading edge of the tenth plate can be seen in the pictures). The investigations of Cur and Sparrow [3] have shown that at this downstream distance fully developed regime is achieved. The interferograms presented in this paper were obtained using the infinite fringe field alignment.

Experimental uncertainities

Flow velocity profiles were measured at three cross sections of the channel upstream of the test section. The measurements were taken by a hot wire anemometer calibrated by a rotameter. From the local measurements of the flow velocities, the cross channel average flow velocity v_m was determined with an estimated accuracy of 7%. The errors connected to the pressure drop measurements were estimated to 6%. The errors in temperature measurements of the top wall and of the heated plates were estimated to 1.5 %. The uncertainities connected to the determination of oscillatory frequencies were 3 %.

Visualized temperature fields

In figure 5, the main heat transfer regions and the characteristic elements of the phenomenon are presented schematically. As the interferometric images, especially due to the instationary nature of the process, contain huge amounts of information, for the evaluation of images and the data reduction procedure both from the aspect of heat transfer and from the aspect of oscillations, it is essential to recognize the most important heat transfer regions and the elements of the image carrying the information on the oscillatory nature of the flow.

Four main regions relevant for the heat transfer analysis can be recognized. In the (i) *top channel region* and the (ii) *bottom channel region* the isotherms are basically parallel with the channel direction, with waves of different wavelength and amplitude travelling in the flow direction.

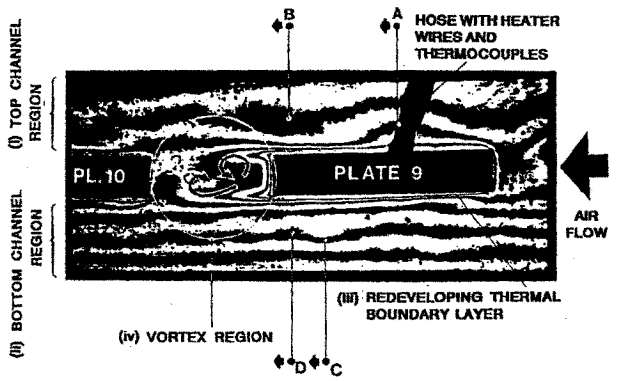

Fig. 5 Schematic of the characteristic regions and values in the investigation of the influence of oscillations on the heat transfer (interferogram recorded at Re = 593.5, plate temperature T_p = 79.6 °C).

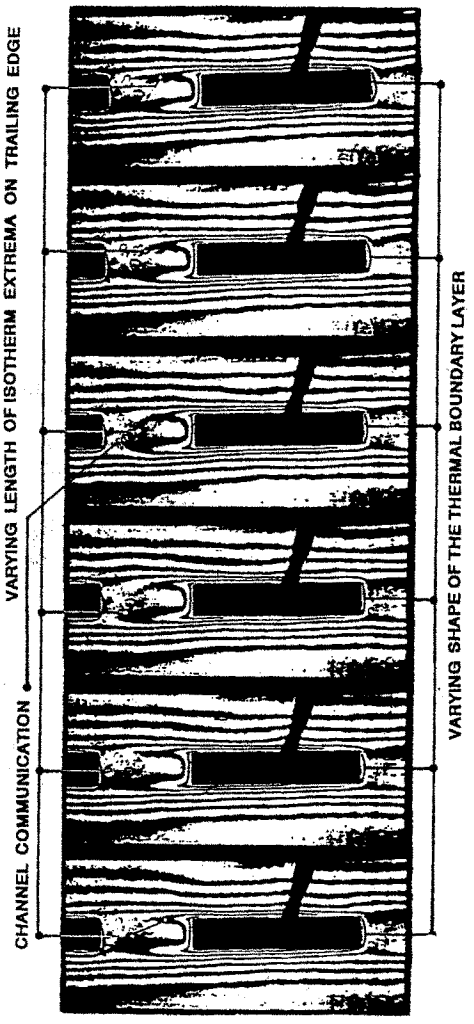

Fig. 6 Sequence of interferograms obtained by high speed cinematography at time instants t = 0, t = 0.01 s, t = 0.02 s, t = 0.03 s, t = 0.04 s and t = 0.05 s (from top to bottom) respectively, recording velocity 400 picture frames per second, Re = 366, temperature of the heated plate T_p = 70 °C. Images were obtained the infinite fringe field alignment and stipes correspond to isotherms (ΔT / fringe pair ca. 2.7 K). The characteristic parameters of the oscillatory behaviour are indicated in the figure.

Waves of short wavelength are often superimposed to the long travelling waves in this region. A certain asymmetry observable in the isotherm width in the top and bottom channel regions is due to buoyancy effects. The (iii) *redevelopment of the thermal boundary layer* can clearly be observed in figure 5. The oscillatory effects in the top and bottom channel regions have a noticable influence on the thickness of the thermal boundary layer causing its successive time varying comprimation and expansion along the plate. This effect is especially pronounced on the leading edge of the plate, originating from the intensive vortex movements in this region. The vortices developing at the trailing edge of the plate — in the region between the two heated plates, (iv) *vortex region* in figure 5 — are responsible for the oscillations of the temperature fields. Their development on plate arrays and their nature was treated in detail in [7], [8], [9]. By measuring the oscillation frequencies of the isotherm extrema in the vortex region, it is possible to determine vortex frequencies, as the time between the successive illuminations is known.

The flow velocity in the experiments was varied stepwise. At Re = 145.2 no oscillations are observable and the temperature fields differ qualitatively only slightly from those obtained at Re = 366 (presented in figure 6), as the information on the oscillatory nature of the process is lost in the stationary reproduction. The situation for Re = 145.2 corresponds to the state also described in [7], [8], [9] (low Reynolds numbers) where two counter rotating vortices are aligned and confined into the inter-plate region due to the strong viscous effects. No communication between the channel flows is visible. Numerical calculations, [7], [8], [9], show that flow velocity profiles in the channel regions are nearly parabolic as for the plane Poiseuille flow situation. At Re = 200 mild oscillations appear, which is in good agreement with the results of the numerical simulations [17].

In figure 6, a temporal sequence of interferograms recorded at Re = 366 is presented. At this Reynolds number the oscillatory behaviour can be observed quite clearly, although the oscillation amplitudes are low. To the channel region isotherms, long, small amplitude waves travelling in the flow direction are superimposed. Under the influence of vortex development, the thermal boundary layer thickness at the leading edge of the plate varies with time. In the vortex region, oscillations of isotherm extrema at the trailing edge of the plate are present together with the communication between top and bottom channels. The oscillatory effects described above are becoming more intensive with increasing Reynolds numbers.

Figure 7 shows an interferogram recorded at Re = 493.4 with higher oscillation amplitudes and more pronounced weaviness of the isotherms in the top and bottom main channel regions compared to the regime presented in figure 6.

In figure 8, a temporal sequence of interferograms for Re = 593.5 is presented. The influence of oscillations on the temperture fields is pronounced. In the top and bottom

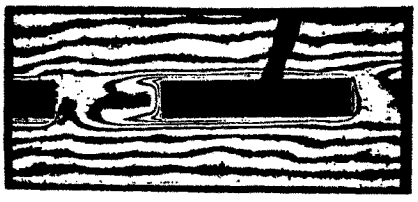

Fig. 7 Interferogram recorded at Re = 493.4

channels short waves superimposed to long waves travelling in flow direction are visible (the superposition is not clearly recognizable in the stationary reproduction and characteristic locations of two travelling maxima are indicated in figure 8) as well as the compression and expansion of the

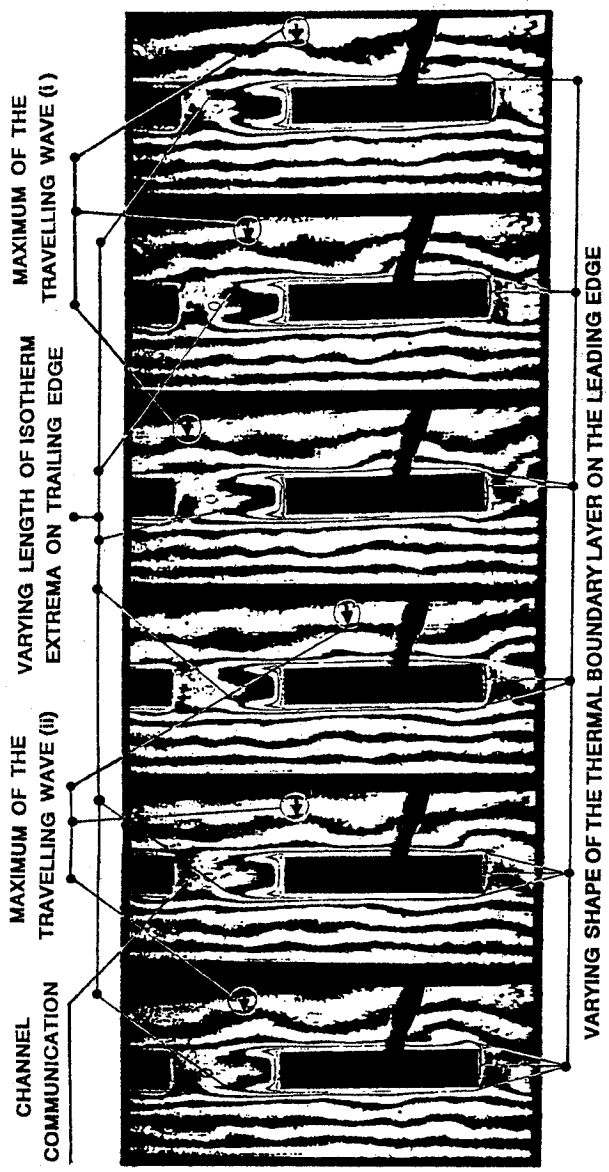

Fig. 8 Sequence of interferograms obtained by high speed cinematography at time instants t = 0, t = 0.005 s, t = 0.01 s, t = 0.015 s, t = 0.02 s and t = 0.025 s (from top to bottom) respectively, recording velocity 600 picture frames per second, Re = 593.5, temperature of the heated plate T_p = 79.6 °C, infinite fringe field alignment. The characteristic parameters of the oscillatory behaviour are indicated in the figure. Arrows indicate the position of two maxima propagating along the top channel region.

thermal boundary layer around the plate and especially on its leading edge. In the vortex region intensive oscillations of isotherm extrema at the trailing edge and intensive communication between top and bottom channel flows are present, also indicated in figure 8. The mechanism of vortex formation for this physical situation is discussed in detail in [7], [8] and [9]. The two counter rotating vortices between the plates are now in unstable configuration, and are alternatively ejected from the inter-plate zone improving communication between the channels and the mixing between vortex region flows and channel flows. The numerical results [17] agree qualitatively very well with the interferometric visualization.

Oscillatory effects

In figure 9, the amplitude of isotherm extrema, determined as indicated in the figure, at Re = 366 (regime in figure 6) in the vortex region versus time is shown, obtained by measuring the locations of isotherm extrema for several periods of oscillations. The basic frequency at Re = 366 is f = 60 1/s.

In figure 10, the amplitude of the isotherm extrema in the upper and lower vortex regions is presented for Re

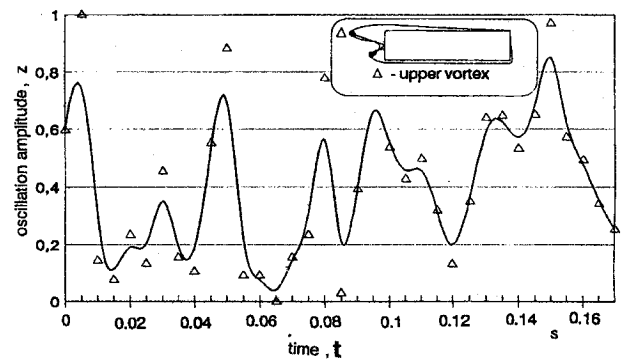

Fig. 9 Amplitude of isotherm extrema in the vortex region at Re = 366 versus time (recording velocity 400 picture frames per second).

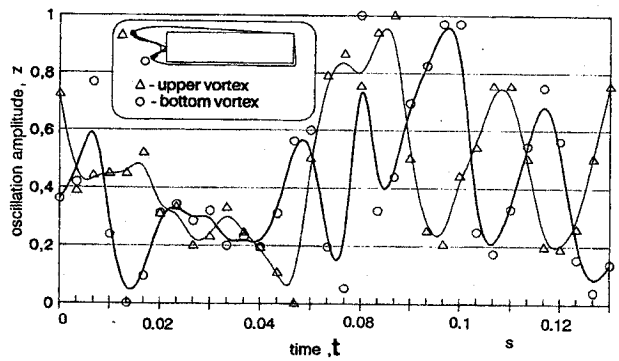

Fig. 10 Amplitudes of isotherm extrema in the vortex region versus time (Re = 593.5, recording velocity 600 picture frames per second).

= 593.5. The oscillatory character can clearly be recognized, characterized with maxima for the upper vortex and minima for the lower vortex, and vice versa. The corresponding main oscillatory frequency is f = 60 1/s.

Pressure drop

Figure 11 shows the ratio of the measured pressure drop Δp and the calculated pressure drop for the basic geomtery Δp_0, a parallel plate duct of height h and fully developed flow. The pressure drop ratio decreases with increasing Reynolds numbers. For Reynolds numbers above 300 it is nearly constant and for a factor of ca. 4.7 above the values obtained for the parallel plate duct.

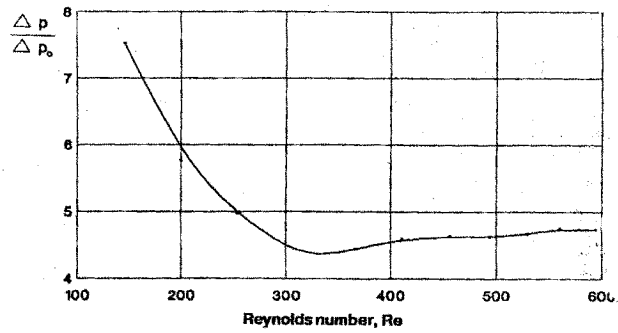

Fig. 11 Pressure drop on the test section scaled by the pressure drop on the basic geometry (parallel plate duct of height h) versus Reynolds number.

Practical significance

The reduction of the size and weight and the increase of the effectiveness of heat transfer equipment is a topic gaining importance in modern heat transfer research. Results obtained by numerical investigation [7], [8], [9] have shown that in communicating channels geometries in the self sustained oscillatory flows significant heat transfer enhancement can be achieved compared to the basic geometry, a parallel plate duct. The experiments presented in the paper verify the existence of the oscillatory effects in the heat transfer process and provide insight into the basic phenomena causing the enhancement, which is important for a better exploitation of these effects. A systematic analysis of heat transfer augmentation with corresponding pressure drop data for a range of geometrical parameters (separation between the channels, periodicity length and groove width) can provide valuable data for design purposes.

CONCLUSIONS

The visualization experiments described in the paper qualitatively verify the results of previous numerical studies [7], [8], [9], but they are not directly quantitatively comparable because of the differing geometrical parameters in the investigated configuration. One important topic of future research is therefore the quantitative comparison of the heat transfer data obtained by numerical techniques and by the evaluation of the visualized temperature fields obtained with interferometry, together with the measurement of overall effects of such enhanced heat transfer surfaces on actual heat exchangers. The experiments presented in the paper show that the self sustained flow oscillations significantly influence the shape of the temperature fields. The onset of oscillations was observed at Re = 200 which agrees with the results of numerical simulations [17].

Heat transfer augmentation in communicating channel geometries is accompanied by increased pressure drops, caused by increased skin friction due to the periodical restarting of the boundary layer and by the creation of the separated flow regions. Pressure drop measurements have shown that by allowing the communication between the channels, the pressure drop increases (compared to the values for the basic geometry), but at higher Reynolds numbers the pressure drop increase remains constant for the investigated range of Reynolds numbers.

NOMENCLATURE

a	—	thickness of the heated plate (figure 1), m
f	—	oscillation frequency in the vortex region, 1/s
h	—	channel height (figure 1), m
l	—	distance between two heated plates (figure 1), m
L	—	period length (figure 1), m
P	—	power supplied to the heater foil, W
Δp	—	pressure drop between entry and exit of the test section, N/m^2
Re	—	Reynolds number
t	—	time, s
T_p	—	plate temperature, °C
v_m	—	cross-channel average flow velocity, m/s
w	—	channel width, m
λ	—	wavelength of laser light, m
ν	—	kinematic viscosity, m^2/s

Subscripts

in	—	refers to channel inlet
out	—	refers to channel outlet
m	—	average value
p	—	refers to plate
0	—	refers to basic geometry (parallel plate duct)

REFERENCES

1. **Bergles, A. E.**, Techniques to augment heat transfer, in Handbook of heat transfer applications, eds. Rohsenow, W. M., Hartnett, J. P., Ganić, E. N., McGraw-Hill, NY, 1985.
2. **Kays, W. M., London, A. L.**, Compact heat exchangers, McGraw-Hill, 1984.
3. **Cur, N., Sparrow, E. M.**, Measurements of developing and fully developed heat transfer coefficients along a periodically interrupted surface, ASME J. Heat Transfer, Vol. 101, pp. 211-216, May 1979.

4. **Kurosaki, Y., Kashiwagi, T., Kobayashi, H., Uzuhashi, H., Tang, S.-C.**, Experimental study on heat transfer from parallel louvered fins by laser holographic interferometry, Experimantal Thermal and Fluid Science, Vol. 1, pp. 59-67, 1988.

5. **Shiina, K., Nakamura, S., Shimizu, N.**, Enhancement of forced convective heat transfer in a rectangular channel using thin-plate-type obstacles, Part 1. Basic characteristics of heat transfer and pressure drop with single phase flow, Scripta Technica, Vol. 2, pp. 9-27, 1989.

6. **Mochizuki, S., Yagi, Y.**, Characteristics of vortex shedding in plate arrays, Proc. 2nd Int. Symp. Flow Visualization, Bochum, West Germany, Sept. 1980.

7. **Amon, K. C. H.**, Heat transfer enhancement and three-dimensional flow by a spectral element-Fourier method, Sc.D. Thesis, MIT, 1988.

8. **Amon, C. H., Mikić, B. B.**, Flow pattern and heat transfer enhancement in self-susteined oscillatory flows, paper AAIA - 89-0428, 27th Aerospace Science Meeting, Reno, Nevada, USA, 1989.

9. **Amon, C. H., Mikić, B. B.**, Numerical prediction of convective heat transfer in self-sustained oscillatory flows, J. Thermophysics, Vol. 4, No. 2, pp. 239-246, 1990.

10. **Nordmann, D.**, Temperatur, Druck und Wärmetransport in der Umgebung kondensierender Blasen, Dissertation, University of Hannover, FRG, 1980.

11. **Mayinger, F., Chen, Y. M.**, Heat transfer at the phase interface of condensing bubbles, Proc. 8 Int. Heat Transfer Conf., San Francisco, California, USA, pp. 1913-1918, 1986.

12. **Ostendorf, W., Mayinger, F., Mewes, D.**, A tomographical method using holographic interferometry for the registration of three dimensional unsteady temperature profiles in laminar and turbulent flows, Proc. 8 Int. Heat Transfer Conf., San Francisco, California, USA, pp. 519-524, 1986.

13. **Snyder, R., Hesselink, L.**, Optical tomography for flow visualization, of the density field around revolving helicopter rotor blade, Applied Optics, Vol. 23, No. 20, pp. 3650-3656, 1984.

14. **Hauf, W., Grigull, U.**, Optical methods in heat transfer, in Advances in Heat Transfer, Vol. 6, Academic Press Inc., New York, 1970.

15. **Mayinger, F., Panknin, W.**, Holography in heat and mass transfer, Proc. 5 Int. Heat Transfer Conf., Tokyo, Japan, pp. 28-43, 1974.

16. **Vest, C. M.**, Holographic interferometry, John Wiley & Sons, New York, 1979.

17. **Amon, C. H.**, Personal communication, 1990.